Modeling and Simulation of Thermal Air Circulation above an Urbanized Area

A. F. KURBATSKY[1] AND L. I. KURBATSKAYA[2]
[1]Institute of Theoretical and Applied Mechanics of Russian Academy of Sciences, Siberian Branch
[1]Department of Physics, Novosibirsk State University
630090 Novosibirsk, Institutskaya Str., 4/1, RUSSIA
[2]Institute of Computational Mathematics and Mathematical Geophysics SB RAS
630090 Novosibirsk, Lavrentiev Avenue 6, RUSSIA
kurbat@nsu.ru

Abstract: - A numerical model to represent the impact of urban buildings on airflow in meso'scale turbulence models is presented. In the model, the buildings are not explicitly resolved, but their effects on the grid-averaged variables are parameterized. An urbanized area is characterized by a horizontal building size, a street canyon width and a building density as a function of height. The improved, three-parametric $E-\varepsilon-\overline{\theta^2}$ turbulence model for the computation of the wind field, air temperature and pollutant dispersion was developed. The transport of momentum, heat and mass under density stratification is evaluated from the fully explicit anisotropic algebraic expressions. These expressions are derived based on the assumption of weak-equilibrium turbulence approach where transport effects on the stresses and heat fluxes are negligible. The heating processes at surfaces of buildings and ground are also modeled. The comparison of the computational results obtained with the present model and existing observational data and numerical models shows that the present model is capable of predicting the structure of turbulence in the urban canopy layer under density stratification and of obtaining high-resolution local wind fields. Numerical experiments with the new three-parametric model show that the behavior of the airflow in the urban canopy layer and above urbanized area is strongly affected by the existence of buildings and thermal stratification, including the urban heat island effect.

Key-Words: - Thermal Convection, Turbulence, Planetary Boundary Layer, Modeling and Simulation

1 Introduction

Urbanization causes drastic changes in radiative, thermal, moisture and aerodynamic characteristics of the land surface, leading to heterogeneities of the airflow. The main reasons for complexity of urban modeling lies in the diversity of spatio-temporal scales over the phenomena occur. In order to compute the mean and turbulent transport, several variables are needed (wind, turbulent coefficients, temperature, pressure, humidity). The numerical models must, indeed, ideally be able to represent the two main scales (the 'urban' and the 'meso') involved. Since the horizontal dimensions of the domain are on the order of the meso'scale (~100 km), to keep the number of grid points compatible with the CPU time cost, the horizontal grid resolution of such (meso'scale) models ranges between several hundreds of meters and a few kilometers. Because is not possible to resolve the city structure in detail (buildings or blocks), but that the effects of the urban surfaces must be parameterized [1]. The most important urban effects on the airflow are: (i) the presence of an intense shear layer at the top of the urban canopy (there, the mean kinetic energy of the flow is converted into turbulent kinetic energy (TKE)); (ii) the development of the turbulent wakes that generated by the roughness elements; efficiently mix and diffuse momentum, heat and mass; (iii) drag due to buildings, i.e. the pressure differences across individual roughness elements; (iv) phenomena of differential heating/cooling of sunlit/shaded surfaces, radiation trapping effects in street canyons and heat storage in buildings can generate the so-called urban heat island effect [2, 3]. (In modeling, the urban heat island effect can be specified by an urban-rural temperature difference. The urban heat island effect may produce major temporal and spatial alterations to the thermodynamics and circulation of the urban airflow).

This study attempts to formulate a three-parametric numerical model for simulation of the air circulation over the urbanized areas. In this model, the turbulent transfer of momentum, heat and concentration in the urban boundary layer is numerically simulated by a time-dependent Rey-

nolds-averaged Navier-Stokes (RANS approach). In the present model, two new ingredients are employed: 1) an updated expression for the pressure-strain correlation, 2) an updated expression for the pressure-temperature correlation. The turbulent momentum and scalar fluxes are determined by the full explicit algebraic expressions which are derived from the closed transport equations for turbulent fluxes and simplified using the weak-equilibrium assumption and symbolic algebra. Closure is achieved by solving the evolution equations for the turbulent kinetic energy, its dissipation rate and scalar variance (the three-parametric turbulence model [1, 4]). This improved meso'scale model is able to reproduce the most important features of a wind field above the city.

Models describing the turbulence to a different degree of completeness and different parameterizations of urban roughness have been used recently to simulate the processes of momentum and heat transfer and pollutant scattering in an urban boundary layer.

For example, in [5], the conventional $E - \varepsilon$ model of turbulence is employed and the effect of stratification on turbulent momentum and heat transfer is taken into account through the methodology of [6], with introduction of corrections for stratification into the proportionality coefficient standing in the standard two-parameter expression for the turbulent viscosity. The shortcomings of this representation are universally known. The turbulent viscosity also depends on the mean-velocity gradient and vertical turbulent heat flux (flux Richardson number) in addition to the turbulent kinetic energy E and its dissipation rate ε. Therefore, the turbulent momentum and heat fluxes are not expressed explicitly in terms of the mean-field gradients and an iteration procedure is required. To take into account the effect of roughness on heat-transfer processes and their influence on urban climate, the governing Navier–Stokes equations and the equation of heat inflow are averaged not only over an ensemble but also over space via introduction of a certain effective-volume function.

Another parameterization scheme [7] uses the approximation of "porous urban roughness," in which the drag and frictional forces induced by buildings of different heights are taken into account in the form of source terms in the equations of motion and heat and moisture inflow via the method proposed in [8]. A scheme of such a parameterization is depicted in Fig. 1b along with a horizontal-wind-velocity profile, which clearly shows the effect of urban roughness on flow in an urban canopy layer. A conventional roughness model and a profile of mean wind velocity are shown in Fig. 1a. The two parameterization schemes are implemented in a simple two-dimensional test of planetary boundary layer (PBL) evolution through a one-parameter model of turbulence in which the turbulent kinetic energy alone is determined from the transport equation. For all turbulent fluxes, the gradient model of the K-theory with the linear turbulent scale regarded as a function of the vertical coordinate alone is used. In this paper, a scheme of parameterization of the roughness of the urbanized surface (Fig. 1b) is also implemented for a simple two-dimensional test.

In our study the modified three-parameter model of turbulence for the PBL over an urbanized surface with modeling of the effect of an urban heat island is used. Unlike the three-parameter model developed previously in [9], for the modified model [1], completely explicit anisotropic models for the turbulent momentum fluxes (Reynolds stresses) and turbulent fluxes of the scalar via symbol algebra are derived.

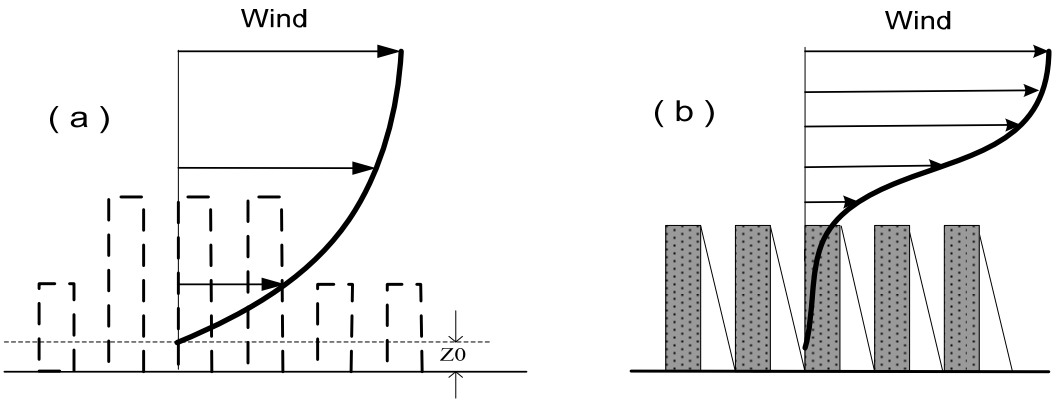

Figure 1. The concept of incorporation of urban canopy model**:** (a) –the conventional model, z_0 - the roughness length; (b) – the urban canopy model.

The model provides additional possibilities for studying the effects of an inhomogeneous underlying surface (thermal and mechanical) on the pattern of a stratified atmospheric flow as compared to one- and two-parameter techniques of modeling the turbulence (see, for example, [5, 7, 10, 11]).

2 The closure turbulence model for planetary boundary layer (PBL)

Both mean and turbulent variables are needed to model a PBL. The following system of partial differential equations models the PBL flow over the urban heat island for a full 24 hour cycle. The Boussinesq approximation for density variations is used to include buoyancy effects:

$$U_x + W_z = 0, \tag{1}$$

$$U_t + UU_x + WU_z = -\frac{\overline{P_x}}{\rho} - \overline{(wu)}_z + fV + D_U, \tag{2}$$

$$V_t + UV_x + WV_z = -\overline{(wv)}_z - fU + D_V, \tag{3}$$

$$W_t + UW_x + WW_z = -\frac{P_z}{\rho} - \overline{(ww)}_z + \beta\Theta g + D_W, \tag{4}$$

$$\Theta_t + U\Theta_x + W\Theta_z = -\overline{(u\theta)}_z - \overline{(w\theta)}_z + D_\Theta. \tag{5}$$

The dependent variables in (1)-(5) are the mean flow velocities U, V, and W in x, y, and z directions respectively, mean pressure P, mean deviation Θ from a reference temperature T_0. The terms D_U, D_V, D_W here represent the forces (e.g., frictional force, drag force etc.) and D_Θ denotes the impact of the sensible heat fluxes from solid surfaces (ground or buildings) on the potential temperature budget. The parametric quantities in the equations (1)-(5) include gravitational acceleration g (9.8 ms^{-2}), Coriolis parameter f (0.8×10^{-4} at latitude 35^0N), volumetric expansion rate of air β (3.53×10^{-3} K^{-1}), and mean air density ρ (1.25 kgm^{-3}). The lower case terms u, v, w, and θ represent time dependent deviations from their respective mean values, and their products in (1)-(5) give the turbulent Reynolds stresses and heat fluxes. They are modeled by the full explicit anisotropic algebraic expressions which are obtained from the differential closed transport equations for turbulent fluxes by reducing them to the system of algebraic equations using the weak-equilibrium assumption. The system of algebraic turbulent flux equations is solved using symbolic algebra (cf. [4]). Three-parametric turbulence model [1, 9] is used to close expressions for the turbulent momentum and scalar fluxes. The turbulent fluxes expressions are not shown here because of their bulkiness.

2.1 Nonlocal expressions for turbulent momentum and heat fluxes

Equations for the turbulent momentum and heat fluxes were solved via symbol algebra. Below, we present expressions for those turbulent momentum and heat fluxes that were used in a numerical test to solve system of equations (1) – (5):

$$\left(\overline{uw}, \overline{vw}\right) = -K_M\left(\frac{\partial U}{\partial z}, \frac{\partial V}{\partial z}\right), \quad \overline{w\theta} = -K_H\frac{\partial\Theta}{\partial z} + \gamma_c,$$

$$K_M = E\tau S_M, K_H = E\tau S_H;$$

$$S_M = \frac{1}{D}\left\{\begin{array}{l} s_0\left[1 + s_1G_H\left(s_2 - s_3G_H\right)\right] + \\ + s_4s_5\left(1 + s_6G_H\right)(\tau\beta g)^2\dfrac{\overline{\theta^2}}{E}\end{array}\right\}$$

$$S_H = \frac{1}{D}\left\{\frac{2}{3}\frac{1}{c_{1\theta}}\left(1 + s_6G_H\right)\right\};$$

$$\gamma_c = \frac{1}{D}\left\{1 + \frac{2}{3}\alpha_2^2G_M + s_6G_H\right\}\alpha_5(\tau\beta g)\overline{\theta^2}$$

is the countergradient term.

The quantities G_H and G_M are defined as

$$G_H \equiv \left(\tau N\right)^2, G_M \equiv \left(\tau S\right)^2,$$

$$N^2 = \beta g\frac{\partial\Theta}{\partial z}, \quad S^2 \equiv \left(\frac{\partial U}{\partial z}\right)^2 + \left(\frac{\partial V}{\partial z}\right)^2,$$

$$D = 1 + d_1G_M + d_2G_H - d_3G_MG_H + d_4G_H^2,$$

$$d_1 = \frac{2}{3}\alpha_2^2, d_2 = \frac{7}{3}\frac{\alpha_3}{c_{1\theta}}, \; d_3 = \frac{2}{3}\alpha_2\frac{\alpha_3}{c_{1\theta\,2}}\;\alpha_5,$$

$$d_4 = \frac{4}{3}\left(\frac{\alpha_3}{c_{1\theta}}\right)^2, \quad s_0 = \frac{2}{3}\alpha_2, \; s_1 = \frac{1}{\alpha_2}\left(\frac{\alpha_3}{c_{1\theta}}\right), \; s_2 = \alpha_2 - \alpha_5,$$

$$s_3 = \alpha_5\left(\alpha_3/c_{1\theta}\right), \; s_4 = \alpha_3\alpha_5, \; s_5 = \alpha_5 + \left(4/3\right)\alpha_2,$$

$$s_6 = \alpha_3/c_{1\theta}, \quad \alpha_1 = \left(4/3\right)\frac{1-c_2}{c_1}, \quad \alpha_2 = \frac{1-c_2}{c_1}, \quad \alpha_3 = \frac{1-c_3}{c_1},$$

$$\alpha_4 = (1-c_{2\theta}), \; \alpha_5 = \left(1-c_{2\theta}\right)/c_{1\theta},$$

(c_1=2, c_2=0. 54, c_3=0.8, $c_{1\theta}$=3.28, $c_{2\theta}$ =0.5).

3 Computational test

The 2D numerical test is carried out. The size of the computational domain is 6×120 km with the resolution of 1 km. The topography is flat with a 10-km wide city surrounded by a rural area. In the model, urban heat island effects are specified by the urban-rural temperature difference. The magnitude of rural-urban temperature difference driving this circulation depends on a variety of factors including the morphology of urban canopy layer. Therefore, the urban roughness parameterization has been incorporated in the improved meso'scale model (Fig. 1b). The ground temperature is the only unsteady boundary condition [1]. This thermal boundary condition simulates the 24 hour cycle of heating by the sun on a land mass located from $x = 0$ km to $x = 120$ km. The meteorological initial conditions are geostrophic wind from the west of 1, 3 and 5m s^{-1}, and atmospheric thermal stratification equal to 3.5 K km^{-1} in potential temperature.

4 Simulation Results

Results of numerical modeling of the urban boundary layer lead to the following conclusions about transformation of the global structure of wind velocity field above the urbanized surface (Fig.1b).

4.1 Turbulent momentum

Comparison of the vertical profiles of local u_* defined as $\left(\overline{uw}^2 + \overline{vw}^2\right)^{1/4}$ with the measurements data are presented in Fig. 2.

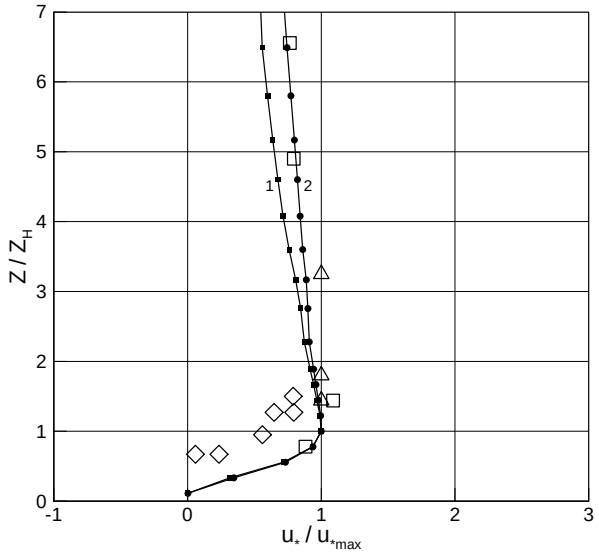

Figure 2. Vertical profiles of the "local" friction velocity u_* (defined as $\left(\langle uw\rangle^2 + \langle vw\rangle^2\right)^{1/4}$) at the center of the urbanized area that are normalized by its maximum value. Different symbols show measurement data: (rhombs) [12-14], (squares) [16], and (triangles) [17]. Lines *1* and *2* correspond to U_G = 3 m/s and U_G = 5 m/s, respectively. The vertical coordinate Z is normalized by the mean height of buildings in the urbanized area Z_H.

Above the roughness sublayer, urban simulations show a region where u_* is nearly constant with height during day and night for both geostrophic wind speeds. In the roughness sublayer the behavior of vertical profile of u_* exhibit a very similar shape as in the observations during night and daytime.

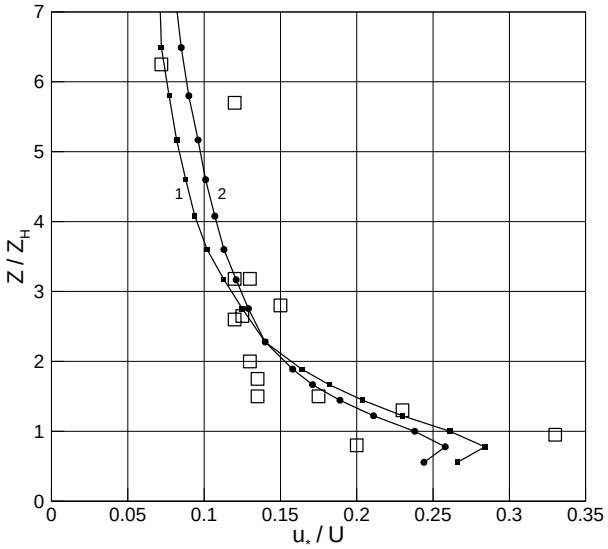

Figure 3. Vertical profiles of the ratio of the local friction velocity u_* to the average horizontal wind velocity at the center of the urbanized area. The symbols correspond to the data of different authors' measurements presented in Fig. 1b of paper [1]. The other notation is the same as in Fig. 2.

The extensive data set of measurements in the cities is presented in review [18] for the ratio of the local friction velocity u_* to the mean velocity of horizontal wind (six groups of data; squares in Fig. 3). The calculated profile of u_*/U (solid line in Fig. 3) has a maximum near the top of the building and then decreases with increasing height, reaching a value close to 0.1 at a height of about a fourfold average height of the building. The profiles calculated for two values of the geostrophic wind (3 and 5 m/s) are in good agreement with observational data.

The simulated results presented in these two figures show that the modified model of turbulence for the PBL and a more realistic model of urban roughness (Fig. 1b) are able to reproduce the vertical pro-

files of both the turbulent momentum flux and the mean velocity of horizontal wind that are consistent with observational data.

4.2 Impact of an urban roughness on the velocity field

It possible to make some quantitative estimation of change of wind speed above the city because influences the mechanical (urban roughness) and thermal (the urban heat island effect) inhomogeneity of the urbanized area. In Fig. 4a, results of the simulation with only the classical Monin-Obukhov similarity theory (MOST) are shown. The simulation with the parameterization of urban roughness in Fig. 4b is represented. From these figures follows, that the urban roughness reduces the wind speed above the city approximately for 24 percent in comparison with

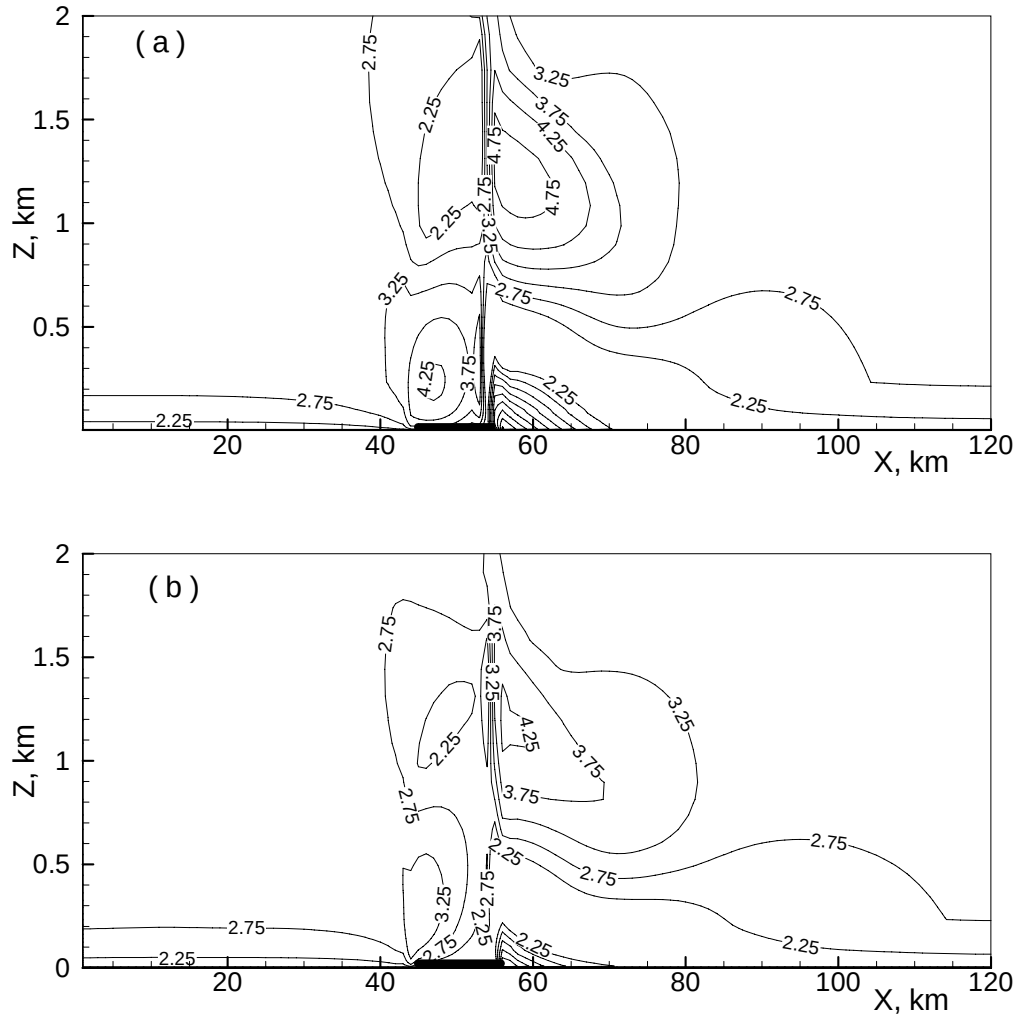

Figure 4. Calculated vertical sections of horizontal wind speed (m/s) for the time 12:00: (a) - simulation with the classical MOST approach and (b) - simulation with the parameterization of urban roughness. The thick line on the abscissa between 45 km and 55 km indicates the location of the urbanized area (city).

the classical MOST approach (Fig. 1a). Thus, the increase of wind speed above the city most likely is connected with the urban heat island effect. The similar modification of wind speed above the city was probably simulated, for example, in [7].

4.3 Turbulent structure of the urban boundary layer

The structure of turbulence in the boundary layer over an urbanized surface is represented by the profile of standard deviation of the vertical velocity (Fig. 5). The profile of standard deviation of the vertical velocity $\sigma_W / u_{*\max}$ is shown by the solid line in Fig. 6 along with the data of measurements (eight data groups) presented in review [18] in their Fig. 2f. These data are depicted by the same symbols (open squares). Fig. 5 shows the modeling results averaged over all calculations during their 24-h cycle.

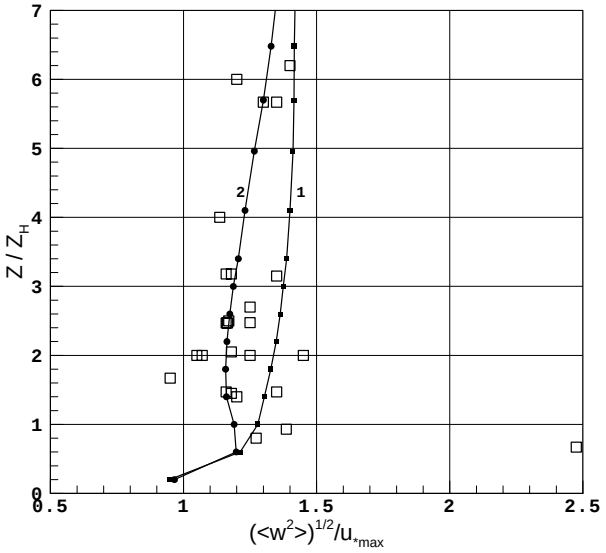

Figure 5. Vertical profile of the standard deviation for the vertical velocity at the center of the urbanized area: simulation at the geostrophic wind speed (*1*) U_G = 3 m/s and (*2*) U_G = 5 m/s. The symbols denote the measurement data from [1].

We note that the calculated profiles are close to the center of the range of data scatter. The normalization is performed with the friction velocity averaged over all values calculated for 24 h. Thus, it may be inferred that, for this structure characteristic of the turbulence field, this PBL model gives results that are in satisfactory agreement with observational data.

4.3 Impact on the dispersion of a passive tracer

The baseline mesoscale model of turbulent atmospheric boundary layer is expanded to include atmospheric dispersion of a passive contaminant by adding equations for mean concentration $C(x_i,t)$, turbulent flux of a contaminant $f_j \equiv < u_i c >$ and correlation $< c\theta >$. Numerical results from validations of differential and algebraic models for turbulent concentration fluxes used in modeling of passive tracer dispersion above an urban heat island under conditions of night-time atmospheric boundary layer (weak wind, stable stratified atmosphere) have shown [19] that the algebraic model for turbulent concentration fluxes provides acceptable in accuracy results. Such a model is formulated in [19] by simplifying closed differential transport equation for the turbulent scalar flux $\langle u_i c\rangle$ under the same local-equilibrium turbulence assumption applied for simplification of equations for turbulent momentum (Reynolds stresses) and heat flux [1].

Anisotropic expressions for vertical $\langle wc\rangle$ and horizontal $\langle uc\rangle$ turbulent fluxes of concentration are derived by means of symbolical algebra in following form,

$$-\langle wc\rangle = \frac{1}{D}\left(\alpha_{1C}\frac{E}{\varepsilon}\left[\langle w^2\rangle + \alpha^*\lambda_1\langle w\theta\rangle\right]\right)\frac{\partial C}{\partial z} + \frac{1}{D}\left(\alpha_{1C}\frac{E}{\varepsilon}\left[\langle uw\rangle + \alpha^*\lambda_1\langle u\theta\rangle\right]\right)\frac{\partial C}{\partial x}, \quad (6)$$

$$-\langle uc\rangle = \frac{1}{D}\left(\frac{E}{\varepsilon}\left[\langle u^2\rangle\lambda_2 + \frac{E}{\varepsilon}\frac{\partial U}{\partial z}\langle uw\rangle + \alpha^*\lambda_1\langle u\theta\rangle\right]\right)\times \frac{\partial C}{\partial x} + \frac{1}{D}\left(\frac{E}{\varepsilon}[\langle uw\rangle\lambda_2 + \frac{E}{\varepsilon}\frac{\partial U}{\partial z}\langle w^2\rangle + \alpha^*\lambda_1\langle w\theta\rangle]\right)\frac{\partial C}{\partial z}. \quad (7)$$

In these expressions, $\alpha^* = (1-\alpha_{2C})/\alpha_{3C}$,

$\lambda_1 = \beta g(E/\varepsilon)$, $\lambda_2 = \alpha_{1C} + \frac{E}{\varepsilon}\frac{\partial W}{\partial z} + \alpha^*\lambda_3\frac{\partial \Theta}{\partial z}$,

$\lambda_3 = \beta g(E/\varepsilon)^2$.

With (6) and (7) the equation for mean concentration

$$\frac{\partial C}{\partial t} + \frac{\partial}{\partial x}CU + \frac{\partial}{\partial z}CW = -\frac{\partial}{\partial z}\langle wc\rangle - \frac{\partial}{\partial x}\langle uc\rangle \quad (8)$$

is reduced to the closed form after neglecting molecular diffusion at higher Reynolds numbers. The numerical constants of diffusion models (6) – (8) are: $\alpha_{1C} = \alpha_{3C} = 3{,}28$, $\alpha_{2C} = 0{,}4$.

A passive tracer is emitted in the city at ground level with a time variation typical of traffic emissions characterized by high values in a morning and low values during night hours in order to reproduce realistic profiles.

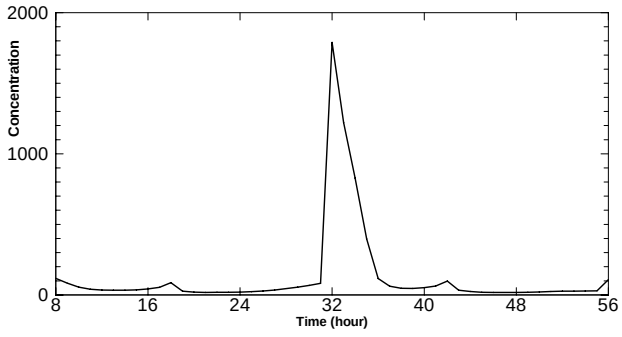

Figure 6. Time evolution of passive tracer surface concentration in the centre of the urban area as computed by the three-parameter turbulence model. Results are for the case with the geostrophic wind $U_G = 3$ m/s.

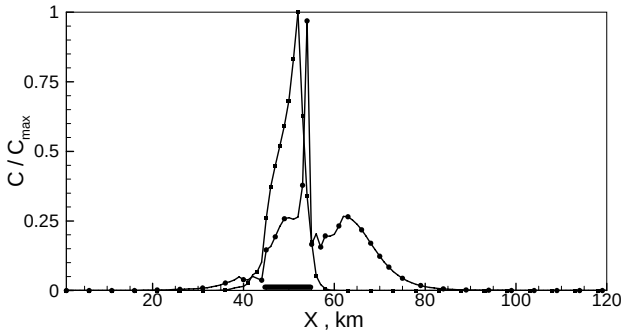

Figure 7. The passive tracer concentration at the lowest level for 13:00 a.m. of the second day. The city is located between 45 km and 55 km. Results are for the case with the geostrophic wind $U_G = 3$ m/s.

The computed tracer concentration in the city centre at the lowest modeled level during 48-hour cycle of simulating the urban boundary layer evolution is presented on fig. 6. As expected, the concentrations are higher during the night than during the day, because the nocturnal boundary layer is much thinner than the diurnal one. It should be noted here that the overprediction of primary pollutants during the night in urban areas, as compared to the measurements, is fairly common for Eulerian photochemical models, especially under low wind conditions [20]. This problem can be linked to an inappropriate reproduction of the nocturnal urban heat island. Distributions of concentration at the lowest level in the centre of the urban area are plotted in Figure 7. As can be seen, at 0700 LST there is an accumulation of tracer concentration (symbols ■ in Figure 7) within the city limits. In addition, by 1300 LST (the second day of modeling) a fixed peak in the distribution of concentration (curve noted by symbols • in Figure 7) forms some distance downwind from the city.

Thus, influence of the urban surface on the day time pollutant concentration away from the city is clearly shown. This result is in qualitative agreement with calculations of [7]. The above-noted behavior of concentration in a vicinity of city's leeward side is caused by the nature of the thermal circulation moved by advection downwind to the leeward side (see also a Figure 8 showing the isotachs of vertical wind speed (arrows show the average wind vector field).

4.4 Countergradient heat flux: comparison between $E-\varepsilon-\overline{\theta^2}$ and $K-\varepsilon$ turbulence models

The two turbulence models commonly used for simulating the urban boundary layer include standard $k-\varepsilon$ model modified for effects of buoyancy on

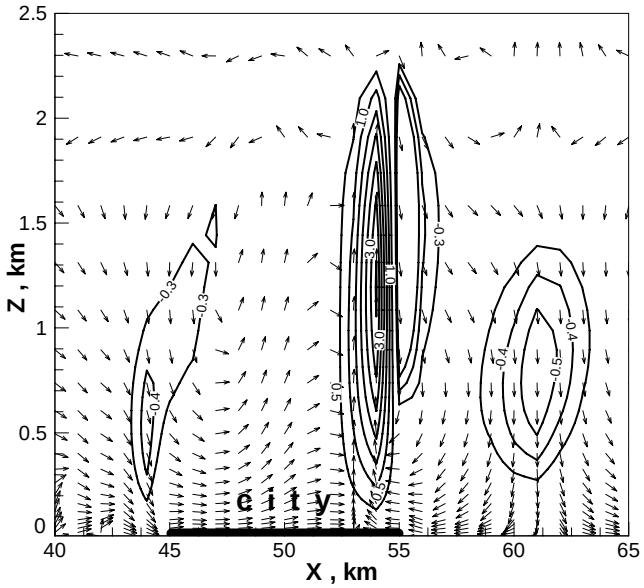

Figure 8. Velocity vectors and isotachs (ms^{-1}) for vertical velocity at 12:00 (*noon*) in the diurnal cycle of simulation for the geostrophic wind speed $\mathrm{U_G} = 3\,\mathrm{m\,s}^{-1}$.

vertical turbulent transport [5], and traditional approach [7] based on the one-parameter turbulence model. Such an approach does not take into account either anisotropic transport in vertical and horizontal directions, or effects of buoyancy on vertical turbulent transport. Computations of velocity vector field, temperature and turbulent quantities inside the urban boundary layer allow detecting differences in the turbulent transport modeled with the three-parameter $E-\varepsilon-\overline{\theta^2}$ model and standard K-theory [7]. For this purpose, values of eddy diffusivities $K_M = -\overline{uw}/(\partial U/\partial z)$ and $K_H = -\overline{w\theta}/(\partial\Theta/\partial z)$ are computed diagnostically and the results are shown in Fig. 9a, b.

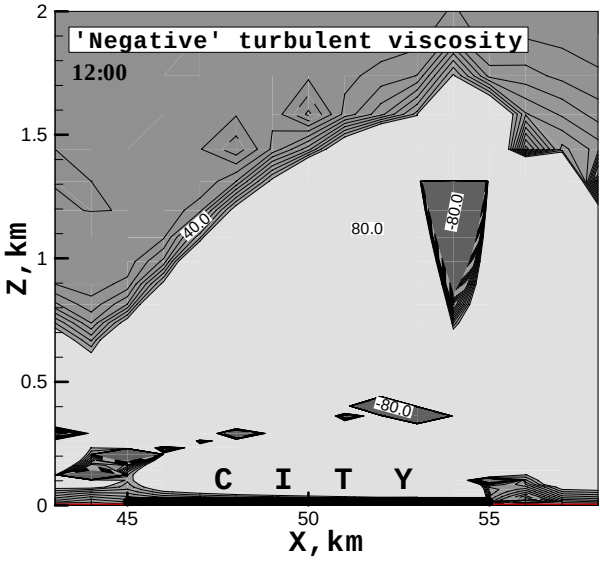

Figure 9a. Eddy diffusivity of momentum for *urban* simulation at noon. Results are for the case with $3\,\mathrm{m\,s^{-1}}$ geostrophic wind.

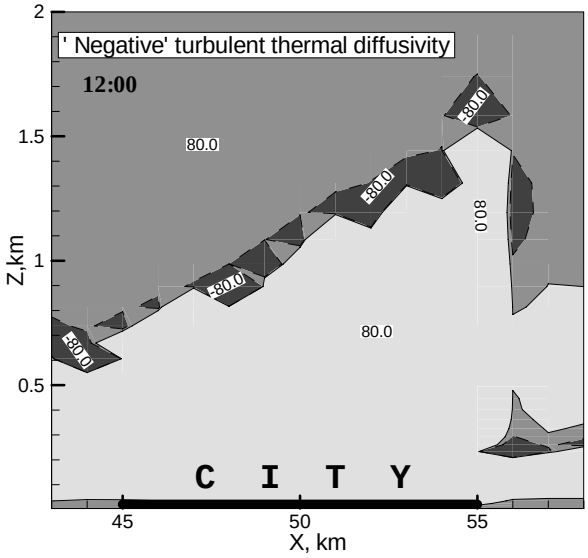

Figure 9b. Eddy diffusivity of heat for *urban* simulation at noon. Results are for the case with $3\,\mathrm{m\,s^{-1}}$ geostrophic wind.

As can be clearly seen in Fig. 9 a, b negative values of K_M and K_H are predicted in the region of turbulent thermal circulation on the leeward side of the urbanized area (Fig. 8). However, their negative values are also predicted in the lower urban boundary layer for K_M and upper urban boundary layer part for K_H. Regions of negative values of K_M and K_H explicitly indicate non-local character of the turbulent transport which can not be described using simple one- or two-parameter turbulence models. In these two models, it is difficult to correctly account for effects of buoyancy on the turbulent transport of momentum, mass and heat. For example, Fig. 10 shows that the 'standard' $\mathrm{k}-\varepsilon$ model underpredicts values of the vertical turbulent heat flux when compared with the $E-\varepsilon-\overline{\theta^2}$ model and fully explicit anisotropic model for turbulent fluxes of momentum, heat and mass.

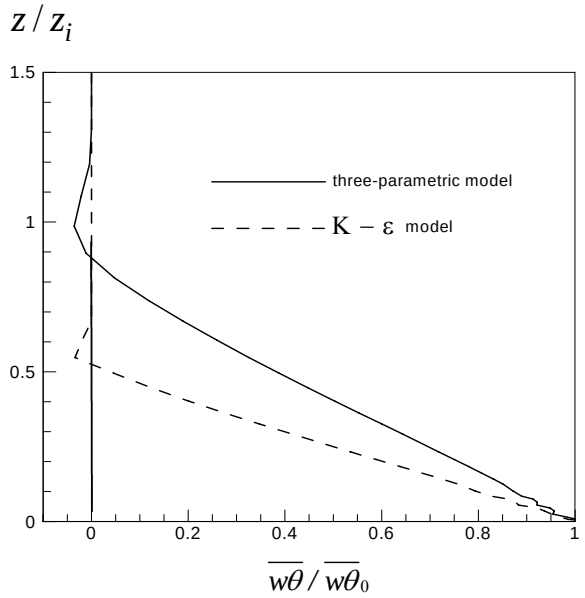

Fig. 10. Vertical turbulent heat flux in a point in the center of the city at 12:00 (*noon*) in the diurnal cycle of simulation for the geostrophic wind speed $U_G = 3\,m\,s^{-1}$ computed by means of 'standard' $k-\varepsilon$ model and the three-parametric $E-\varepsilon-\overline{\theta^2}$ turbulence model with the fully explicit anisotropic model for turbulent fluxes. The fluxes normalized on the maximum value of $\overline{w\theta}_0$, z_i is the inversion layer height.

5 Conclusion

A three-parameter mesoscale model of explicit anisotropic turbulent fluxes of momentum and heat has been developed in this paper for modeling atmospheric flows over an inhomogeneous underlying surface. An important property of the model lies in the improvement of estimating the processes of transfer in the vertical and horizontal directions under different stratification conditions, which are usually observed in an urban boundary layer.

A simple two-dimensional numerical test on the influence of mechanical factors (urban roughness) and thermal factors (effect of an urban heat island) on a global structure of the atmospheric boundary layer has been implemented.

This test has shown that the results of numerical simulation are in good qualitative and quantitative agreement with the data of field measurements. The model is able to reproduce turbulent processes within the urban canopy layer and above it with satisfactory accuracy.

The formulated nonlocal model of turbulent fluxes can be potentially used to model the atmospheric boundary layer within the "urban" scale and "mesoscale." It is clear that a realistic modeling of the dispersion of urban pollutants requires an accurate knowledge of meteorological parameters for this region of the urban boundary layer, where the pollutants are emitted and where people live. An efficient use of this model for the turbulent PBL requires the specification (from measurement data) of "input" parameters such as the vertical distributions of the three base functions of the model, E, ε, and $\langle\theta^2\rangle$ (for example, in the morning hours for a stably stratified

PBL). Testing the potentials of the RANS turbulence model for an urban PBL requires the measurement data on the distributions of a number of quantities, such as the variance of the vertical component of turbulent velocity and the boundaries of surface and raised inversions (including those under the conditions of weakened PBL turbulence in the night and early-morning hours, measurement data on vertical distributions of temperature, turbulent heat flux, TKE, and other parameters).

The improvement of the model requires a more accurate calculation of heating processes at surfaces of buildings and ground, and this modification of the model is regarded as the aim of our further study. Note that the description of a detailed pattern of urban climate requires of surface temperatures modeling from the urban energy balance model.

Acknowledgements

This study was supported by the Russian Foundation for Basic Research (project No. 06-05-64002).

References:

[1] A.F. Kurbatskii and L. Kurbatskaya, Three-Parameter Model of Turbulence for the Atmospheric Boundary Layer over an Urbanized Surface, *Izvestia, Atmospheric and Oceanic Physics, No. 4,Vol.42, 2006, pp.439-455*.

[2] R. D. Bornstein and T. R. Oke, Influence of pollution on urban climatology, *Adv. Environ. Sci. Engrg.,* Vol. 2, 1981, pp. 171-202.

[3] R.D. Bornstein. Mean Diurnal Circulation and Thermodynamic Evolution of Urban Boundary Layers, *In: Modeling the Urban Boundary Layer, American Meteorological Society, Boston, MA,* 1987, pp.53-94.

[4] Y. Cheng, V. M. Canuto and A. M. Howard, An Improved Model for the Turbulent PBL, *J. Atmos. Sci.,* Vol. 59, 2002, pp. 1500–1565.

[5] T.C. Vu, Y. Ashie and T. Asaeda, A Turbulence Closure Model for the Atmospheric Boundary Layer Including Urban Canopy, *Boundary-Layer Meteor.* Vol. 102, 2002, pp. 459– 490.

[6] B. E. Launder, On the Effects of Gravitational Field on the Turbulent Transport of Heat and Momentum, *J. Fluid Mech.* Vol. 67, 1975, pp. 569–581.

[7] A. Martilli, A. Clappier and M.W. Rotach, An Urban Exchange Parameterization for Mesoscale Models, *Boundary-Layer Meteor.* Vol. 104, 2002, pp. 261–304.

[8] M. R. Raupach, R. A. Antonia, S. Rajagoplan, Rough-Wall Turbulent Boundary Layers, *Applied. Mech. Rev*., Vol. 44, 1991, pp. 79–90.

[9] A.F. Kurbatskii, Computational modeling of the penetrative convection above the urban heat island in a stably stratified environment, *J. Appl. Meteor.,* Vol. 40, 2001, pp. 1748-1761.

[10] A. C. Benim, F Gul, E. Pasqualotto, RANS Predictions of Turbulent Flow Past a Circular Cylinder over the Critical Regime, *Proc. of 5th IASME/WSEAS International Conference on FLUID MECHANICS and AERODYNAMICS (FMA'07)*, pp.235-240.

[11] S. H. Sohrab, A Modified Theory of Turbulent Flow over a Flat Plate, *Proc. of 5th IASME/WSEAS International Conference on FLUID MECHANICS and AERODYNAMICS (FMA'07)*, pp.71-79.

[12] M. W. Rotach, Turbulence within and above an Urban Canopy. ETH Dissertation, No. 9439, 1991.

[13] M. W. Rotach, Turbulence Closure to a Rough Urban Surface. Part I: Reynolds Stress, *Boundary-Layer Meteor*., Vol. 65, 1993a, pp. 1–28.

[14] M. W. Rotach, Turbulence Closure to a Rough Urban Surface. Part II, *Boundary-Layer Meteor*., Vol. 65, 1993b, pp. 1–28.

[15] M. W. Rotach, Profiles of Turbulence Statistics in and above an Urban Street Canyon, *Atmos. Environ*., Vol. 29, 1995, pp. 1473–1486.

[16] S. Oikawa, Y Meng, Turbulence Characteristics and Organized Motion in a Suburban Roughness Sublayer, *Boundary-Layer Meteor*., Vol. 74, 1995, pp. 289–312.

[17] C. Feigenwinter, The Vertical Structure of Turbulence above an Urban Canopy, *PhD Thesis,* University of Basel, 1999, 76 pp.

[18] M. Roth, Review of atmospheric turbulence over cites, *Q. J. R. Meteor. Soc.,* Vol. 126, 2000, pp. 941-990.

[19] A. F. Kurbatskii, L.I. Kurbatskaya, Numerical investigation of the urban heat island: verification of the Eulerian atmospheric diffusion models, *Atmos. Oceanic Opt.,* No. 5-6, Vol. 17, 2004, pp. 417-424.

[20] N. Moussiopoulos, P. Sahm, K. Karatzas, S. Papalexiou, K. Karagianndis, Assessing the impact of the new Athens airport to urban air quality with contemporary air pollution models, *Atmos. Environ.,* No. 10, Vol. 31, 1997, pp. 1497-1511.